

Alma Mater Studiorum Università di Bologna
Archivio istituzionale della ricerca

Similarity of catchment dynamics based on the interaction between streamflow and forcing time series: Use of a transfer entropy signature

This is the final peer-reviewed author's accepted manuscript (postprint) of the following publication:

Published Version:

Neri M., Coulibaly P., Toth E. (2022). Similarity of catchment dynamics based on the interaction between streamflow and forcing time series: Use of a transfer entropy signature. JOURNAL OF HYDROLOGY, 614(Part. B), 1-14 [10.1016/j.jhydrol.2022.128555].

Availability:

This version is available at: <https://hdl.handle.net/11585/900836> since: 2024-02-22

Published:

DOI: <http://doi.org/10.1016/j.jhydrol.2022.128555>

Terms of use:

Some rights reserved. The terms and conditions for the reuse of this version of the manuscript are specified in the publishing policy. For all terms of use and more information see the publisher's website.

This item was downloaded from IRIS Università di Bologna (<https://cris.unibo.it/>).
When citing, please refer to the published version.

(Article begins on next page)

This is the final peer-reviewed accepted manuscript of:

Mattia Neri, Paulin Coulibaly, Elena Toth, Similarity of catchment dynamics based on the interaction between streamflow and forcing time series: Use of a transfer entropy signature, Journal of Hydrology, Volume 614, Part B, 2022, 128555, ISSN 0022-1694, <https://doi.org/10.1016/j.jhydrol.2022.128555>.

The final published version is available online at:

<https://doi.org/10.1016/j.jhydrol.2022.128555>

Terms of use:

Some rights reserved. The terms and conditions for the reuse of this version of the manuscript are specified in the publishing policy. For all terms of use and more information see the publisher's website.

This item was downloaded from IRIS Università di Bologna (<https://cris.unibo.it/>)

When citing, please refer to the published version.

1 **Similarity of catchment dynamics based on the interaction between streamflow and forcing** 2 **time series: use of a transfer entropy signature**

3 Mattia Neri¹, Paulin Coulibaly², Elena Toth¹

4 ¹ DICAM, University of Bologna, Bologna, Italy

5 ² McMaster University, Hamilton, Canada

6 *Correspondence to:* Mattia Neri (mattia.neri5@unibo.it)

7 **Abstract**

8 The transfer of the hydrological information between catchments is founded on the definition of hydrological similarity,
9 which is in turn strictly connected to the features to be regionalised. In order to characterise the catchment behaviour in
10 the streamflow generation processes, the similarity should reflect also the interaction between meteorological forcings
11 and river streamflow time series. While previous hydrological research has identified basins with similar meteorological
12 forcings (i.e. similarity of climate) or with similar streamflow time-series (i.e. similarity of runoff response), the present
13 work proposes, for the first time, to quantify the interaction between the entire time-series of different forcing data and
14 streamflow observations, to be considered as a novel hydrological signature and used as a catchment similarity metric.

15 In particular, the present study proposes the use of a multi-variate entropy-based measure, the so-called *transfer entropy*,
16 a time-asymmetric quantity which analyses the interaction between different signals. The concept of transfer entropy is
17 applied for identifying the dominant hydrological processes occurring in a catchment, measuring the transfer of
18 information from different meteorological forcings over the catchment to the corresponding observed time series of daily
19 streamflow at the basin outlet. The resulting transfer entropy values are then used as signatures to characterise the main
20 catchment dynamics, and a classification of the basins region is obtained assuming that similar values of transfer entropy
21 correspond to hydrologically similar basins.

22 The methodology is tested on a densely-gauged set of more than 200 catchments across Austria and the outcomes of the
23 approach are evaluated against a set of morpho-climatic catchment attributes and typical streamflow signatures.

24 Despite the limitations, the method is able to distinguish the predominant or partial role of snow melt and
25 evapotranspiration across the dataset, helping to assess differences in catchment response time and to highlight the role
26 of very high orographic precipitation in catchments with a dominant snow regime. The study demonstrates the potential
27 of transfer entropy as complementary to consolidated streamflow signatures for assessing hydrological similarity and for
28 quantifying the connection between different catchment processes.

29 **Keywords:** Catchment similarity; Hydrological signatures; Catchment classification; Information flow in streamflow
30 generation dynamics; Information Theory; Transfer entropy.

31 **1 Introduction**

32 The assessment of catchment similarity has always been addressed as one of the essential steps for transferring
33 information between watersheds, through the identification of the dominant hydrological processes and their main
34 characteristics. The delineation of similar groups of basins is required for several regionalisation applications (Rosbjerg
35 et al., 2013). It can be implemented, for instance, for improving regional flood frequency analysis (e.g. Castellarin et al.,
36 2001; Merz and Blöschl, 2005; Rao and Srinivas, 2006; Sikorska et al., 2015), for assessing water availability at annual

or seasonal scale (e.g. Berghuijs et al., 2014; Holmes et al., 2002; Viglione et al., 2007) or for low flow statistics estimation (e.g. Laaha and Blöschl, 2006; Vezza et al., 2010).

Most of the studies implement indices and signatures based on streamflow observations as metrics for characterising the hydrological behaviour of the watersheds, looking at the similarity between some of the hydrograph features (e.g. Archfield et al., 2014; Jehn et al., 2020; McManamay and Derolph, 2019; Sawicz et al., 2011; Yaeger et al., 2012). In the case of ungauged basins, climatic and morphological characteristics are typically used instead (e.g., among the many others, Knoben et al., 2018; Swain and Patra, 2019) to identify similarity.

On the other hand, when the transfer of hydrological information regards the streamflow generation processes at fine temporal scale, it is essential to capture the sequential order and the stochastic nature of the runoff generation and propagation, considering the information content embedded in the entire streamflow hydrograph and also in its forcings. To address this issue, a few recent studies have focused on different classification metrics that may synthesise the temporal correlation structure of streamflow processes: some of them proposed to analyse similarity of runoff temporal dynamics through the parameters of linear models estimating the global autocorrelation function (ACF) of the streamflow time series (Chiang et al., 2002; Corduas, 2011; De Thomas and Grimaldi, 2001; Grimaldi, 2004); others used single autocorrelation coefficients for regionalisation purposes (e.g. Castiglioni et al., 2010; Lombardi et al., 2012; Montanari and Toth, 2007). More recently, notable contributions were given by Singh et al. (2016), who used a “data depth” function to explore similarity of the whole dynamics of streamflow time series for the transfer of rainfall-runoff model parameters, or by Pérez Ciria and Chiogna (2020) who applied a classification framework based on the analysis of daily streamflow at multiple temporal scales with the Discrete Wavelet Transform. Alternatively, functional analysis can be used to represent different hydrological regimes as functions which enable the exploitation of the full information stored in the time series of annual hydrograph when clustering catchments (e.g. Brunner et al., 2020).

By taking into account the characterisation of the forcing time-series as well as that of the hydrograph, Toth (2013) provided the first ever watershed clustering including measures of the fine time-scale variability and correlation structure of both rainfall and streamflow series, including a correlation scaling exponent to classify the shape of the hydrograph ACFs, but such indices are obtained independently for each of the two time series.

To the best of our knowledge, no studies have so far considered the *interaction* between the entire time series of forcing data (e.g. precipitation, evapotranspiration and snow melt) and streamflow, quantifying it through signatures to be used as clustering metrics. Such additional signatures may be effective to enhance the assessment of the similarity of the main hydrological processes taking place in different watersheds, and in particular for better understanding the controls of the streamflow generation dynamics.

Linear cross-correlation analysis, which measures the correlation of two time series as functions of the displacement (in time) of one relative to the other, may measure the similarity of different forcings and streamflow signals in order to identify the dominant factors guiding the runoff generation. However, given the high nonlinearity of the rainfall-runoff relationship, the use of a metric able to look beyond linear correlation analysis between meteorological inputs and streamflow would be required. One of the possible approaches for this purpose is the use of the concepts of *Information Theory* (Shannon, 1948): they are based on the notion of *entropy*, i.e. the content of information of a signal (as a time series), or, in the multivariate case, the content of information shared between more variables (i.e. *mutual information*). An entropy-based measure particularly suitable for our purposes is the so-called *transfer entropy* (Schreiber, 2000), a time asymmetric quantity which analyses the interaction between different signals.

Information theory-based approaches have been widely used in hydrology and water resources during the last few decades. Singh (1997) reports a first detailed overview of the development of these methods, describing typical

applications in hydrological sciences. They range, for instance, from the optimal design of river monitoring networks (e.g. Alfonso et al., 2014; Foroozand and Weijs, 2021; Keum et al., 2017) and from geostatistics (Thiesen et al., 2020) to quantitative precipitation estimation (Neuper and Ehret, 2019). While Ben Jaafar and Bargaoui (2020) showed that mutual information between precipitation and streamflow time-series may be linked to the robustness of a conceptual hydrological model, a few recent studies made use of entropy terms derived from Shannon's information theory for identifying hydrological similarity. For example, Rajsekhar et al. (2013) used *direction information transfer* (a standardised version of mutual information) to group hydrological units with similar drought severity and duration. Ridolfi et al. (2016) proposed an entropy-based approach to define homogeneous regions based on the redundant and total information provided by pairs of hydrometric stations. Loritz et al. (2018) made use of normalised mutual information between the simulated streamflow time series of sub-catchments nested within the same downstream catchment for clustering hillslope models into functional groups of similar runoff generation, and implemented Shannon entropy as measure of diversity in simulations. On the same line, Ehret et al. (2020) included entropy concepts in adaptive clustering to simplify and reduce the computational effort of a distributed hydrological model. Such studies applied the entropy concepts for grouping and characterising discharge (or model states) time series across the considered study regions. More interestingly for the present study, Bennett et al. (2019) demonstrated how the above cited quantity called *transfer entropy* can be used to quantify the active transfer of information between hydrologic processes at various time scales. While they quantified the flow of information between hydro-climatic controls and streamflows aiming at evaluating the structure of different hydrological models, in the present study the concept of transfer entropy is applied instead for identifying the processes controlling streamflow generation at catchment scale. In a first step, the different amount of information transferred from the three main meteorological forcings driving the water balance (i.e. precipitation, snow melt and actual evapotranspiration) to observed runoff is quantified in terms of transfer entropies. For all the study watersheds the estimated transfer entropy values are then used as signatures to characterise the governing catchment dynamics. In order to better interpret the spatial pattern of the results, a classification of the basins is finally implemented assuming that similar values of transfer entropy for the three forcings identify similar basins, through a simple hierarchical clustering algorithm. The methodology is tested on a large and densely gauged dataset of 206 Austrian catchments. The resulting values of transfer entropy and the obtained clusters are analysed and discussed against the values of catchment attributes and against a set of typical streamflow signatures. The purpose of the present study is to test the potential of transfer entropy for characterising and classifying catchment dynamics as a complement to traditional runoff signatures and flow indices. In particular, the aim is to explore the ability of the novel signature to capture different aspects of the streamflow generation dynamics, providing a further measure for the assessment of hydrological similarity. The paper is organised as follows: Sec. 2 introduces the concept of transfer entropy. Sec. 3 presents the study region and data. Sec. 4 gives the details about the methodology used for characterising the basins based on the information flow from meteorological forcings to runoff, and Sec. 5 reports the corresponding results. Finally, Sec. 6 reports an interpretation of the obtained transfer entropy values and classes and Sec. 7 gives the concluding remarks on the approach.

2 Entropy theory and transfer entropy

Information theory was initially developed in the field of communication engineering. In information theory, entropy quantifies the uncertainty derived from the probability of occurrence associated to a variable, measuring the extent of

117 surprise of a particular outcome. By extension, entropy is a measure of the amount of information content in a generic
 118 signal. Shannon entropy, $H(X)$, provides a mathematical formula for explaining the information content of a variable X
 119 (e.g. the streamflow time series at a given gauge), which has a set of discrete probabilities, p_1, \dots, p_n (Shannon, 1948;
 120 Singh, 1997). The average information content associated to X is called *marginal entropy* and it is given as:

$$H(X) = - \sum_{i=1}^n p(x_i) \log_2 p(x_i) \quad (1)$$

121 where n is the total number of class intervals (also called bins) representing the possible states of the variable, and $p(x_i)$
 122 is the occurrence probability of X in the i th class interval. Strictly speaking, assuming that one bit is the information
 123 content of a binary random variable that is 0 or 1 with equal probability, Shannon's entropy measures the number of bits
 124 needed to optimally encode a sequence of realisations of X . If, for instance, X is a constant signal (i.e. it has a unique
 125 known value) the probability of that event (i.e. the probability that X assumes the constant value) will be one, while all
 126 the other probability will be zero; in this case there will be no uncertainty associated to X , and the information content
 127 $H(X)$ will be zero. On the other hand, if X has a uniform distribution (i.e. the probability of each event is equal to $1/N$)
 128 the marginal entropy assumes its maximum at $\log_2 N$, since:

$$H(X) = - \sum_{i=1}^n \frac{1}{N} \log_2 \frac{1}{N} = N \frac{1}{N} \log_2 N \quad (2)$$

129 In the multivariate case, the *joint entropy* represents the whole amount of information embedded in more variables. In
 130 case of two signals X and Y , it is defined as follows:

$$H(X, Y) = - \sum_{i=1}^n \sum_{j=1}^m p(x_i, y_j) \log_2 p(x_i, y_j) \quad (3)$$

131 The marginal entropies of a number of signals often contain duplicated information, so that the joint entropy should be
 132 less than the sum of marginal entropy unless every variable is independent of each other (Keum et al., 2017).
 133 Consequently, it is possible to measure the portion of the information content shared between the two variables X and Y ,
 134 that is named *mutual information* (Cover and Thomas, 2005):

$$I(X, Y) = H(X) + H(Y) - H(X, Y) \quad (4)$$

135 Mutual information quantifies the knowledge we gain about Y by measuring the variable X , or vice versa. Conditional
 136 forms of the above presented measures of information can be also defined. The *conditional entropy*, i.e. the additional
 137 information provided by the entire time series X if we already know the information content of Y , is given by:

$$H(X|Y) = H(X) - H(X, Y) \quad (5)$$

138 Similarly, *conditional mutual information*, given a third variable Z , can also be defined as the information content shared
 139 between X and Y , provided we already know the information content of Z :

$$I(X, Y|Z) = H(X|Z) + H(Y|Z) - H(X, Y|Z) \quad (6)$$

140 All the above mentioned quantities are symmetrical, except for the choice of the conditioning variables. They are not
 141 describing the flow of information between variables; in other words, we do not know if a variable is somehow influencing
 142 the others and vice versa.

143 Schreiber (2000) developed a method for accounting for information transfer, which considers the flow of information in
 144 time between signals. In order to do so, the variables are artificially “shifted” in time: given two original variables X_t and
 145 Y_t , let's consider X_{t-lx} and Y_{t-ly} as new time series, built by shifting X_t and Y_t respectively by lx and ly time lags. The
 146 quantity, called *transfer entropy*, can be written as a particular case of conditional mutual information:

$$TE_{X \rightarrow Y}(lx, ly) = I(Y_t, X_{t-1}, \dots, X_{t-lx} | Y_{t-1}, \dots, Y_{t-ly}) \quad (7)$$

where $TE_{X \rightarrow Y}$ is the transfer entropy from X to Y associated to time lags lx and ly : it represents the mutual information between the target variable Y at time t and the dependent variable X at all the previous lx time lags, conditioned by the knowledge of the history of variable Y itself at the previous ly time lags (in case of zero lag, it would lose its “directional” nature, corresponding to the simple mutual information between X and Y). More intuitively, transfer entropy can be thought of as the additional knowledge we gain about the variable Y at time t by measuring X at the previous lx time steps, with respect to the information already given by knowing the previous ly states of Y . It quantifies the effective information flow from X to Y , given fixed time lags.

For a more rigorous treatment and definition of transfer entropy, see Schreiber (2000). The reader can find other applications of transfer entropy as a tool for causal effects estimation, for instance, in Ruddell and Kumar (2009), who used it for quantifying information flows within ecohydrological systems, or in Hlinka et al. (2013), who employed transfer entropy to estimate causality of climate networks.

It has been underlined in the literature that, when choosing the values of the two time lag parameters lx and ly , there is a trade-off between computational complexity and estimation of accuracy and stability (Schreiber, 2000). Hlinka et al. (2013) showed how the reliability of transfer entropy estimate decreases for increasing values of time lag, due to the difficulties in the estimation of high-dimensional probability distributions.

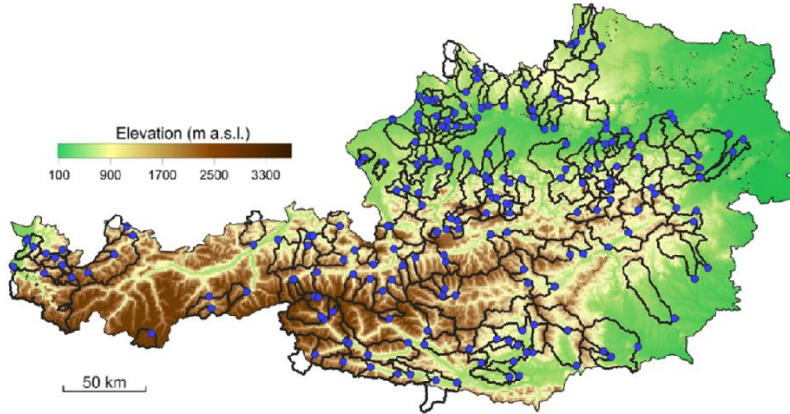
3 Study region and data

The study region is Austria, where data for 206 catchments (see Figure 1), covering a large portion of the country, are available. The size of the watersheds varies considerably, but mainly under 1000 km² (93% of the basins), and none of them exceeds 3000 km². The topography of the country varies significantly from the flat and hilly area in the north-east to the Alps in the centre and in the south-west, particularly steep in the extreme west. The annual precipitation ranges from about 600 mm in the east, where the evaporation plays an important role in the water balance, to more than 2000 mm in the west, mainly due to orographic lifting of north-westerly airflows at the rim of the Alps (Viglione et al., 2013). Even if the amount of precipitation and evapotranspiration ranges consistently, the aridity index (here defined as the ratio between annual potential evapotranspiration and precipitation) assumes values from 0.2 to 1, meaning that the all the watersheds are mainly wet or weakly arid and annual evapotranspiration is never higher than precipitation (i.e. there are no energy-limited basins, following Budyko, 1974). Land use is mainly agricultural in the lowlands and forest in the medium elevation ranges. Alpine vegetation and rocks prevail in the highest catchments (Parajka et al., 2005).

Data were provided by the Institute of Hydraulic Engineering and Water Resources Management (Vienna University of Technology), which previously screened the runoff data for errors and removed all stations with significant anthropogenic effects. Hydro-meteorological data include daily streamflow and daily meteorological time series for the 33-year period 1976-2008: daily average precipitation, temperature and potential evapotranspiration are defined for 200-meter elevation zones for all the study catchments (for further detail about the meteorological time series, see Parajka et al., 2005). The potential evapotranspiration is estimated by a modified Blaney–Criddle method (Parajka et al., 2003) using interpolated daily air temperature and grid maps of potential sunshine duration (Mészáros et al., 2002).

In addition to hydro-meteorological data, a set of further morphological and climatic catchment attributes were also made available in order to characterise the basins and to analyse the results of the methodology: topographic attributes such as mean catchment elevation and mean slope, derived from a 1x1 km digital elevation model; climatic features such as mean and aridity index and snow fraction of precipitation were instead derived from climatic input time series, while average

185 snow depth was interpolated from the vast snow gauge network covering the country. The upper portion of Table 1 reports
 186 a summary of the presented basin descriptors, along with their main statistics across the study region.



187
 188 **Figure 1.** Austria, the study area. Blue points refer to stream gauges and black lines to gauged catchment boundaries.

189 **Table 1.** Catchment attributes (above) and considered signatures (below).

Code	Description	Unit	Min	Median	Max
<i>Elev</i>	Mean elevation	m a.s.l.	287	915	2964
<i>Slope</i>	Mean slope	m/m	0.9	12.4	28.5
<i>MAP</i>	Mean annual total precipitation	mm	675	1230	2310
<i>Aridity</i>	Aridity index (PET/MAP)	-	0.21	0.46	0.96
<i>SnowFr</i>	Fraction of precipitation fallen as snow (i.e. precipitation fallen in days below 0°)	-	0.06	0.17	0.60
<i>SnowD</i>	Mean annual snow depth	cm	1	14	68
\overline{Q}_y	Mean annual specific runoff	mm/yr	170	795	2617
ΔPar	Range of the Parde's coefficients	-	0.38	1.23	3.12
<i>lowQ</i>	Normalised low flow statistic	-	0.02	0.27	0.63
<i>highQ</i>	Normalised high flow statistic	-	1.58	2.66	4.08
<i>flashiness</i>	Flashiness index (Baker et al., 2004)	-	0.04	0.19	0.63
<i>BFI</i>	Baseflow index (Gustard et al., 1992)	-	0.23	0.66	0.93

190
 191 In order to describe the streamflow characteristics of the basins in the study region, a set of streamflow signatures is also
 192 computed. Six widely applied signatures describing flow regimes at different time scales across the same Austrian dataset
 193 (summarised in the lower portion of Table 1) are here considered to support the interpretation of the outcomes of the
 194 proposed approach:

- 195
 - mean annual specific runoff (mm/yr) \overline{Q}_y which estimates the overall water availability of a catchment, defined
 196 as the average daily specific runoff Q_d during the period of record of length T :

$$\overline{Q}_y = \frac{365}{T} \sum_{t=1}^T Q_d(t) \quad (8)$$

- 197
 - the range of the Pardé's coefficients Par_i (-), defined as the mean monthly runoff \overline{Q}_i for month $i = 1, \dots, 12$
 198 divided by the mean annual runoff \overline{Q}_y ; this signature is an indicator of runoff seasonality: since each of Parde's
 199 coefficient refers to the deviation of monthly runoff in respect to the annual average, their variability
 200 ΔPar estimates how the runoff is distributed along the year:

$$\Delta Par = \max\left(\frac{\bar{Q}_t}{\bar{Q}_y}\right) - \min\left(\frac{\bar{Q}_t}{\bar{Q}_y}\right) \quad (9)$$

- normalised low flow statistic *lowQ* (-), calculated as the value of daily runoff $Q_{95\%}$ (mm d⁻¹) which is exceeded the 95% of the time, divided by the mean daily runoff;
- normalised high flow statistic *highQ* (-) calculated as the value of daily runoff $Q_{5\%}$ (mm d⁻¹) which is exceeded the 5% of the time, divided by the mean daily runoff;
- the runoff *flashiness*, calculated by the Richards–Baker flashiness index (Baker et al., 2004), which is the ratio of the sum of the absolute values of the day-to-day fluctuations of streamflow Q_d relative to the total flow during the period of record of length T :

$$flashiness = \frac{\sum_{t=1}^T |Q_d(t) - Q_d(t-1)|}{\sum_{t=1}^T Q_d(t)} \quad (10)$$

- the baseflow index *BFI*, i.e. the proportion of baseflow to total streamflow. Baseflow is commonly considered “as the portion of flow that comes from groundwater storage or other delayed sources” (Hall, 1968), i.e. water that has previously infiltrated into the soil and recharged to aquifers but can also originate from other sources of delayed flow (e.g. snowmelt). Here, baseflow is estimated through the IH-UK (Institute of Hydrology, UK) smoothed minima approach (Gustard et al., 1992; Natural Environment Research Council, 1980), a two-component hydrograph separation approach based on progressively identified streamflow minima.

The spatial pattern of the catchment characteristics and of the considered streamflow signatures will be reported later in the paper to better discuss the outcomes of the proposed approach (Figure 6).

4 Methods: catchment characterisation with transfer entropy

The aim of the study is to show the use of transfer entropy (TE) as a catchment attribute for identifying dominant hydrological processes and for the characterisation of different types of catchment dynamics.

In this experiment, we decided to consider the information flow transferred to the observed daily streamflow time series, from the observed daily precipitation and from the other two main components responsible for the runoff generation: daily actual evapotranspiration and snow melt. Such forcings have been chosen due to their dominant impact on the water balance, similarly to what done for example also by Berghuijs et al. (2014), but unfortunately they are not directly measurable and have therefore been estimated through hydrological modelling (see Sec. 4.1).

The approach we propose in this work is based on the following hypotheses: i) for each catchment the flow of information between catchment forcing data (the main controls of runoff generation, i.e. rain, snow melt and actual evapotranspiration) and the observed streamflow can be quantified with its transfer entropy, ii) if two or more catchments have similar values of such information flow (similar quantities of transferred information from each of the forcings), they are similar and the streamflow generation mechanisms are dominated by similar processes.

This section describes the methodology of the proposed approach. First, actual evapotranspiration and snow melt time series are estimated through the application of a rainfall-runoff model. Then, transfer entropy (TE) values from precipitation, actual evapotranspiration and snow melt are computed for all the study catchments. In order to better capture and interpret the spatial pattern of the TE values and to understand the potential of the proposed signature, a simple hierarchical clustering algorithm is finally applied for grouping the basins according to the three values of transfer entropy.

4.1 Estimation of snow melt and actual evapotranspiration through rainfall-runoff modelling

As introduced previously, two of the variables considered as sources of information to be transferred to catchment streamflow are actual evapotranspiration (*AET*) and snow melt. As in many previous studies (e.g. Berghuijs et al., 2014; Sikorska et al., 2015; Tarasova et al., 2020), these quantities have been modelled, since they are very difficult to measure. For this purpose, it was decided to use the TUW model, which was found to behave very well in Austria (see e.g. Merz and Blöschl, 2004; Neri et al., 2020; Parajka et al., 2005). The TUW model is a semi-distributed version of the HBV model (Bergström, 1976; Lindström et al., 1997) developed by Viglione and Parajka (2018), and available through the R-package *TUWmodel* (for further details about model routines and characteristics the reader can refer to, e.g., Merz and Blöschl, 2004; Neri et al., 2020).

The model is run at daily time step for all the study catchments, with the semi-distributed model structure obtained by dividing them into 200-meter elevation zones. While model daily inputs (precipitation, temperature and potential evapotranspiration) and model states are defined over such zones, the 15 model parameters are assumed to be the same for the entire catchment (additional details on the parameterisation are given in Appendix B).

The TUW model is used in the present work exclusively for modeling the actual evapotranspiration and snow melt at daily scale. It should be noted that the model is calibrated against the observed runoff and the resulting simulated snow melt and actual evapotranspiration values are therefore not fully independent from the flow observations; however, such relationship is indirect, being due only to the model parameters values, and it should not affect the analysis of the information transfer.

The resulting simulation performances in terms of Kling-Gupta (KGE) and Nash-Sutcliffe efficiency (NSE), calculated on the streamflow values and summarised in Table 2, are very good with KGE ranging from 0.56 to 0.94. Despite the limitation of using simulated forcings, the fact that the TUW model is confirmed to perform very well on all the Austrian catchments seems to support the assumption that it may be able to adequately simulate also the snow melt and *AET* values.

Table 1. TUW performances: values of the 10% (q10), 50% (med.) and 90% (q90) quantiles for Kling-Gupta (KGE) and Nash-Sutcliffe (NSE) efficiencies.

	q10	med.	q90
KGE (-)	0.78	0.85	0.91
NSE (-)	0.60	0.71	0.81

4.2 Computation of transfer entropy

Having simulated through the model the actual evapotranspiration and snow melt time series, the flow of information from catchment forcing data to the observed streamflow is quantified, computing the transfer entropy (TE) from each of the three daily time series of:

- precipitation (*P*)
- actual evapotranspiration (*AET*)
- snow melt (*melt*)

to the observed streamflow (*Q*).

The use of the transfer entropy introduced in Sec. 2 (Eq. 7) requires the preliminary choice of the values of the time lags l_x and l_y to be used in the computation. As stated above, high time lags negatively influence the reliability of the

estimates, due to problems in the estimation of high-dimensional probability distributions. In order to minimise these effects, but also to keep the methodology as simple as possible for evaluating the potential of transfer entropy in the characterisation of rainfall-runoff dynamics, in this study it was decided to consider only the previous time step ($lx = ly = 1$), thus assessing the information transfer between the forcing variable at day $t - 1$ and the streamflow at day t . It is of course clear that the target variable (i.e. daily streamflow time series Q) is influenced by the forcing variables (P , AET and $melt$) also at time lags greater than one day, due to the *memory* of the hydrological processes occurring in the basin. This is a strong limitation, in particular when analysing the role of the actual evapotranspiration, since the proposed approach can not capture the long-term response of the watershed. However, choosing to consider just one lag allows us to have at least a first order estimate of the impact of the different variables on the streamflow, and at the same time to simplify the TE calculation, for a better understanding of the information flow. Thus, for this parameterisation, the transfer entropies (from Eq. 7) for the three independent variables are defined as:

$$TE_{P \rightarrow Q}(1,1) = I(Q_t, P_{t-1} | Q_{t-1}) \quad (11a)$$

$$TE_{AET \rightarrow Q}(1,1) = I(Q_t, AET_{t-1} | Q_{t-1}) \quad (11b)$$

$$TE_{melt \rightarrow Q}(1,1) = I(Q_t, melt_{t-1} | Q_{t-1}) \quad (11c)$$

The computation of transfer entropy is carried out within the R Programming Environment (R Core Team, 2019), by using the package *RTransferEntropy* (Behrendt et al., 2019).

Transfer entropy, as every information theoretic measure, requires the estimation of probabilities of occurrence. Such estimate, which is a potential source of uncertainty, can be performed following various techniques. One option is the use of continuous distribution functions (e.g. Krstanovic and Singh, 1992), and in the case of multivariate data the choice of the distribution is limited to a normal or lognormal distribution, for which joint entropy can be calculated as a function of the covariance matrix (Ozkul et al., 2000), otherwise no equations are available to estimate multivariate entropy quantities. Alternatives are, for instance, the use of non-parametric density estimators (e.g. Mishra and Coulibaly, 2009) or the use of discrete probability distributions which define a number of class intervals to approximate the probabilities by the corresponding relative frequencies.

Entropy calculations using discrete distributions have been preferred in the recent specialised literature, due to the unavoidable assumptions when choosing a specific distribution function and to the above mentioned difficulties in formulating the joint entropy in many distributions (Fahle et al., 2015). However, the discrete entropy term calculations also require an assumption of data quantisation and there is no consensus on which method should be used (Keum and Coulibaly, 2017). Among the simplest methods, for example, the *histogram method* divides the range of the variables in class intervals with equal width, while the *quantile method* uses fixed quantiles as bin boundaries and it is based on the notion that you want to have the tail events (i.e., extreme events) in separate bins. In general, the choice of the intervals/quantiles should be guided both by the distribution of the data and by the number of observations.

In this case, Behrendt et al. 2019 recommend that the number of bins is limited, in order to avoid too many zero observations when calculating relative frequencies as estimators of the joint probabilities in the transfer entropy equations. The default version of the algorithm sets the bin limits to the 5% and 95% quantiles, isolating extreme tail events. On the other hand, the literature on the use of transfer entropy for purposes similar to our analysis is extremely limited, and, to the best of our knowledge, no reference on the quantisation method is provided. For this experiment, the effect of different bin widths and types was tested in analyses preceding the present experiment, but the results (not reported here) were inconclusive: as expected, the binning strategy affects in part the TE calculations and consequently the resulting basin classification. However, this is consistent with the previous findings of Keum et al. (2017) and Keum and Coulibaly

(2017), which demonstrated how the quantisation method altered the outcomes of other information theory-based applications, in that specific case for the optimal design of hydrometric networks.

In the absence of additional guidelines, it was finally decided, acknowledging some subjectivity in such choice, to divide the data interval into five bins based on the quantile method defining a large central interval between the quartiles, and dividing the tails of the distribution into two intermediate intervals (between 5% and 25% and between 75% and 95% quantiles respectively) and two “extreme” intervals (outside the 5% and 95% quantiles).

Another limitation of the methodology is given by the fact that transfer entropy estimates are known to be biased due to small sample effects. To address this issue, the comparison of the results with those obtained as a benchmark with a shuffling procedure may be used. Shuffled versions of the independent variable $X_{shuffled}$ can be generated, by randomly drawing values from the time series of X and realigning them to generate new time series; then, the corresponding “shuffled” transfer entropies can be computed $TE_{X_{shuffled} \rightarrow Y}$: this procedure “destroys” the time series dependencies of X , as well as the statistical dependencies between X and Y , and it thus introduces a “white noise” against which the calculated transfer entropy can be benchmarked. The implemented R tool allows the automatic computation of the *effective transfer entropy* (Marschinski and Kantz, 2002): in order to derive a consistent estimator, shuffling is repeated many times and the average of the resulting shuffled transfer entropy estimates across all replications of $\overline{TE}_{X_{shuffled} \rightarrow Y}$ is subtracted from the Shannon transfer entropy to obtain a bias corrected estimate:

$$ETE_{X \rightarrow Y} = TE_{X \rightarrow Y} - \overline{TE}_{X_{shuffled} \rightarrow Y} \quad (12)$$

The number of shuffles is here set to 100. More details may be found in the *RTransferEntropy* documentation (Behrendt et al., 2019).

In this paper, transfer entropy is always computed in the effective form of Eq. 12. However, for the sake of simplicity, we will in the following refer to the three quantities by the terms $TE_{P \rightarrow Q}$, $TE_{AET \rightarrow Q}$ and $TE_{melt \rightarrow Q}$ (where the lag specification is also omitted and it is always 1).

The computation of transfer entropy values is carried out for all the catchments in the dataset and for the three forcing variables. At the end of the process each watershed is characterised by three values of transfer entropy which estimate the information transferred from each of the control variables to the observed runoff.

4.3 Catchment classification based on transfer entropy

The proposed approach assumes that catchment similarity can be associated to the amount of information flow transferred from the different runoff generation components (i.e. basins with similar values of transfer entropy are assumed to be hydrologically similar). Thus, the last step of the methodology is the implementation of a clustering algorithm to group the Austrian catchments based on the set of their transfer entropy values. As mentioned previously, this additional step allows us to better understand the meaning of the proposed transfer entropy (TE) signatures and of their interrelationship, merging the spatial pattern of the three new measures into a unique outcome. The classification is here named TE-HC (Transfer Entropy - Hierarchical Clustering).

Distances between catchments are calculated as the Euclidean distance in the three-dimensional transfer entropy space and their classification is performed using a hierarchical cluster analysis based on Ward’s minimum variance method (Ward, 1963). Even if the recent literature proposes more refined and sophisticated classification algorithms and procedures, several studies still use it for grouping catchments based on signatures with satisfactory results (e.g. Jehn et al., 2020; Kuentz et al., 2017). Ward’s clustering is a simple algorithm which minimises the total within-cluster variance. At the first step, each item represents a single cluster. Then, at each step, the algorithm finds the pair of clusters that leads

345 to minimum increase in total within-cluster variance after merging. This is recursively repeated until all the items belong
346 to one single cluster. Hierarchical cluster analysis has the advantage that it does not require the a priori definition of the
347 number of clusters. The algorithm produces a classification tree and the number of clusters is chosen only in a second
348 phase by “cutting” the tree.

349 5 Results

350 5.1 Transfer entropy values and correlation with morpho-climatic attributes and streamflow signatures

351 Figure 2 reports the results of the transfer entropy computation described in Sec. 4.2 above. It shows the spatial pattern
352 of the estimated information flow from the three control variables to observed runoff across the Austrian basins ($TE_{P \rightarrow Q}$
353 in panel a, $TE_{AET \rightarrow Q}$ in panel b and $TE_{melt \rightarrow Q}$ in panel c); below, a histogram for each of the three TE component reports
354 the distribution of the values across the range of variability of TE. It can be observed that $TE_{P \rightarrow Q}$ reaches so much higher
355 values (up to 0.20 bits) and the distribution is more uniform; on the other hand, the distribution of $TE_{AET \rightarrow Q}$ and $TE_{melt \rightarrow Q}$
356 is positively skewed and the ranges of variability are more limited: maximum information flow values do not exceed 0.10
357 and 0.7 bits, respectively for *AET* and *melt*. It is important to specify (not showed in the figure) that $TE_{P \rightarrow Q}$ is negatively
358 correlated with the other two components (Pearson's linear correlation coefficients around -0.30), while $TE_{AET \rightarrow Q}$ and
359 $TE_{melt \rightarrow Q}$ are strongly and positively correlated between each other (Pearson's coefficient equal to 0.78).

360 In order to ease the interpretation of the results, the scatterplots of each of the three obtained TE against the morphological
361 and climatic features of Table 1 are reported in Figure 3, where the number inside each plot indicates the corresponding
362 significant Pearson's correlation coefficients (if the correlation is not significant, i.e. p-values above 0.05, the coefficient
363 is omitted). The results indicate that all the three entropy components are clearly related to the attributes linked to elevation
364 (*Elev*, *Slope*, *SnowF* and *SnowD*), while only $TE_{AET \rightarrow Q}$ and $TE_{melt \rightarrow Q}$ show relationships with climatic attributes (*MAP*
365 and *Aridity*); however, the interpretation of the results will be deepened in the next sections.

366 The relationships between the single TE values and the set of streamflow indices described in Sec. 3 are also investigated.
367 As mentioned in the introduction of the paper, streamflow signatures synthesise in indexes different flow conditions and
368 aspects of the hydrographs. Here the purpose is to look for any potential relationships between such measures and the
369 transfer entropies which, on the other hand, represent the interaction between forcing variables and runoff.

370 Thus, the six streamflow signatures presented in Table 1 are computed for the entire dataset using all the available
371 streamflow records. While their spatial pattern will be reported in the next section (bottom panel of Figure 6) when
372 compared to the TE-HC outcomes, here Figure 4 shows the scatterplots between the five signatures and the three transfer
373 entropy values. Again, the corresponding Pearson's correlation coefficients are reported in case the test is significant (p-
374 value below 0.05).

375 Detailed discussion and interpretation of the TE values against catchment attributes and signatures will be given in Sec.
376 6.

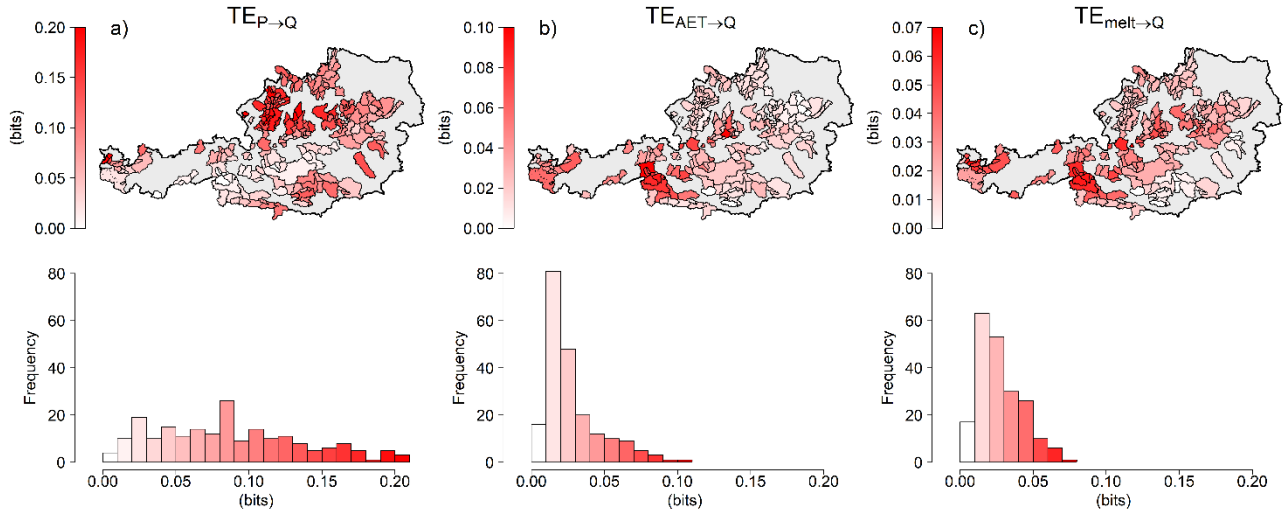


Figure 2. Computed transfer entropy values: spatial pattern of estimated information flow from a) precipitation, b) actual evapotranspiration and c) snow melt to the streamflow (above), and corresponding distributions of the values inside the range of variability (histograms below).

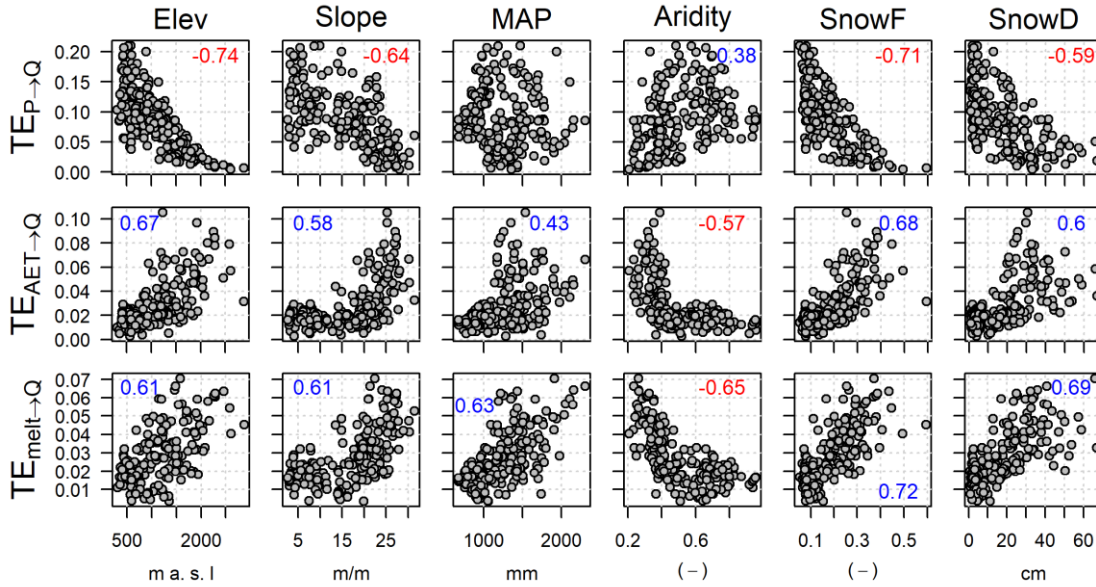


Figure 3. Values of transfer entropy against morpho-climatic catchment attributes across Austria: mean basin elevation (*Elev*), mean basin slope (*Slope*), mean areal precipitation (*MAP*), aridity index (*Aridity*), fraction of precipitation falling as snow (*SnowF*) and mean snow depth (*SnowD*). Numbers inside each plot indicate significant Pearson's correlation coefficients (for p-values above 0.05, the coefficient is omitted).

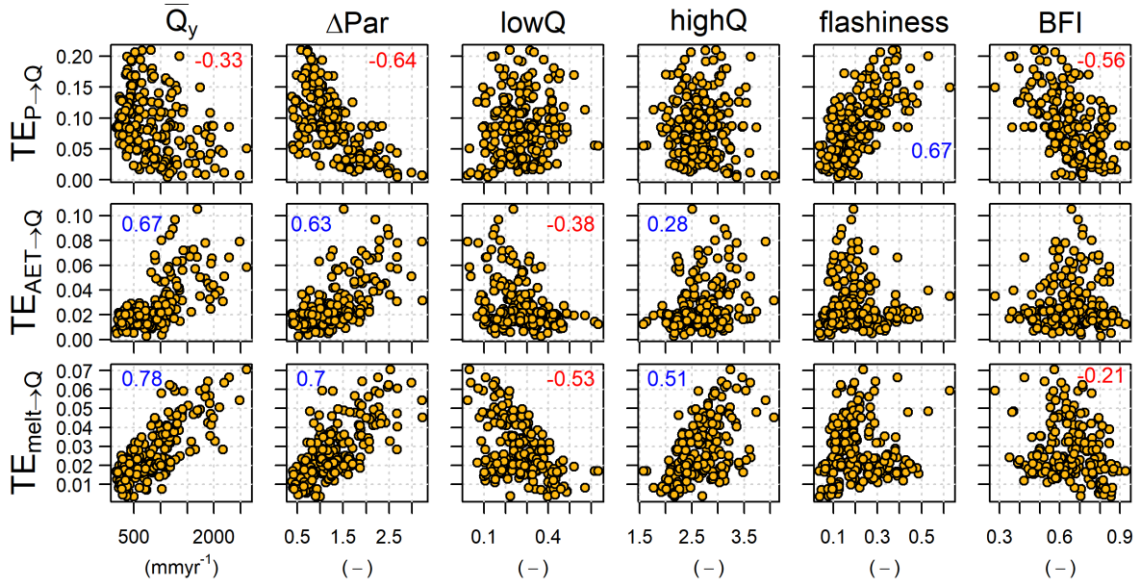
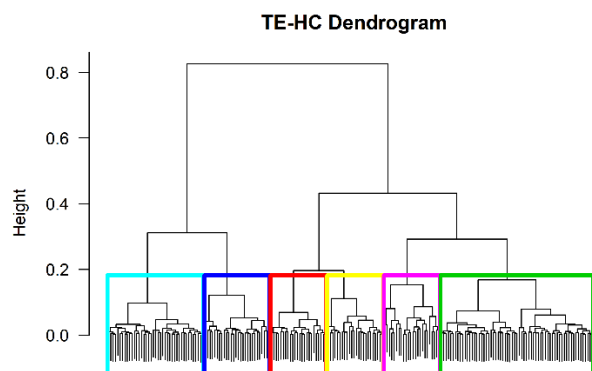


Figure 4. Values of transfer entropy against streamflow signatures: mean annual runoff (\bar{Q}_y), runoff seasonality (Range of the Pardé's coefficients ΔPar), low flow statistic ($lowQ$), high flow statistic ($highQ$), flashiness index ($flashiness$) and baseflow index (BFI). Numbers inside each plot indicate significant Pearson's correlation coefficients (for p-values above 0.05, the coefficient is omitted).

5.2 TE-HC classification

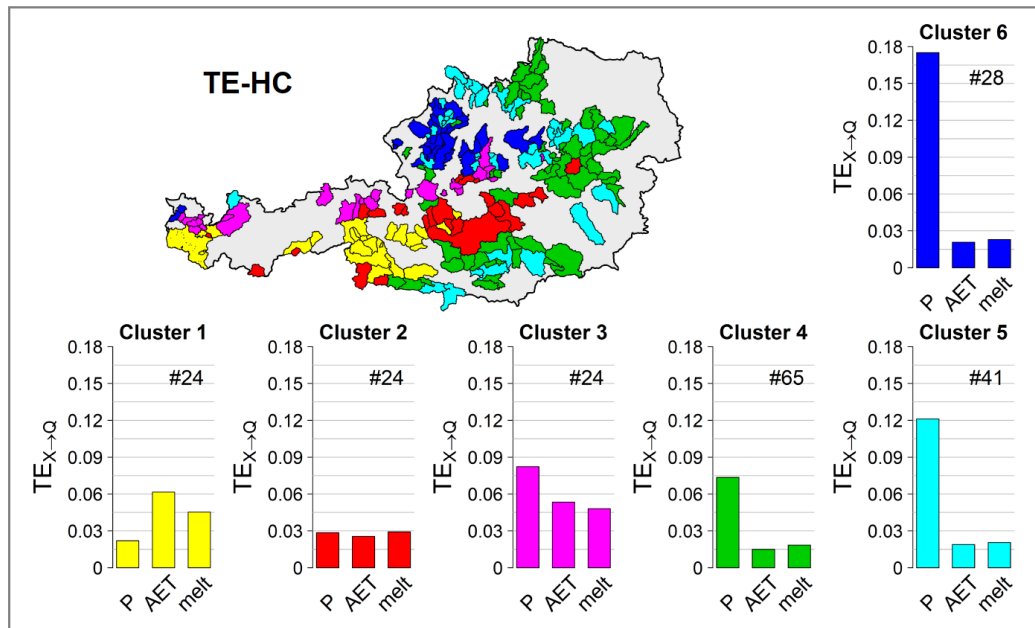
This section shows the results of the TE-HC classification (Sec. 4.3). The TE-HC dendrogram, showed in Figure 5, reports the hierarchical relationships between the basins during the classification process: it is a diagram representing the classification tree produced by the algorithm when applied on the sets of three TE values for each catchment. The vertical axis of the graph represents the “height” (i.e. dissimilarity) between clusters, while the horizontal axis represents the catchments (names are omitted to simplify the graph, given the high number of items). At the beginning of the classification process (at the base of the tree) each basin represents a single cluster; moving upward, the graph shows how the algorithm finds successively the clusters leading to minimum increase in total within-cluster variance, and recursively merges them. Here, a number of clusters equal to six is considered suitable to properly visualise the spatial pattern of the combined new TE values. The six clusters, highlighted by the coloured rectangles, are generated by cutting the classification tree of Figure 5.

The upper portion of Figure 6 shows a map of the Austrian catchments, coloured accordingly to the clusters they belong to. All around the map a bar plot for each cluster (identified by the same color) shows the average transfer entropy values of the cluster basins. Below in the same figure, the TE-HC classification is compared to the spatial pattern of the selected morpho-climatic catchment attributes (panels a-f) and streamflow signatures (panels g-m), described in Sec. 3. Finally, Figure 7 shows the variability of the different basin attributes and streamflow signatures across the obtained clusters.



407

408 **Figure 5.** TE-HC dendrogram: classification tree illustrating the arrangement of the clusters produced by the algorithm. Catchment
 409 names at the base of the tree are omitted. Vertical axis refers to the dissimilarity ("height") between catchments and clusters.
 410 Horizontal axis refers to catchments. Coloured rectangles identify the six considered clusters.



411

412

413

414

415

416

Figure 6. Upper panel: TE-HC classification results; the colour of basin drainage areas refer to the cluster they belong to; the bar plots show the average transfer entropy values for the clusters and for each independent variables; the size of the sample is also reported on the bar plots. Bottom panels: pattern of morphological and climatic catchment attributes (elevation (a), slope (b), MAP (c), aridity index (d), snow fraction (e), snow depth (f)) and streamflow signatures (mean annual runoff (g), range of Pardé's coefficients (h), low flow statistic (i), high flow statistic (l), flashiness index (m) and baseflow index (n)) across Austria.

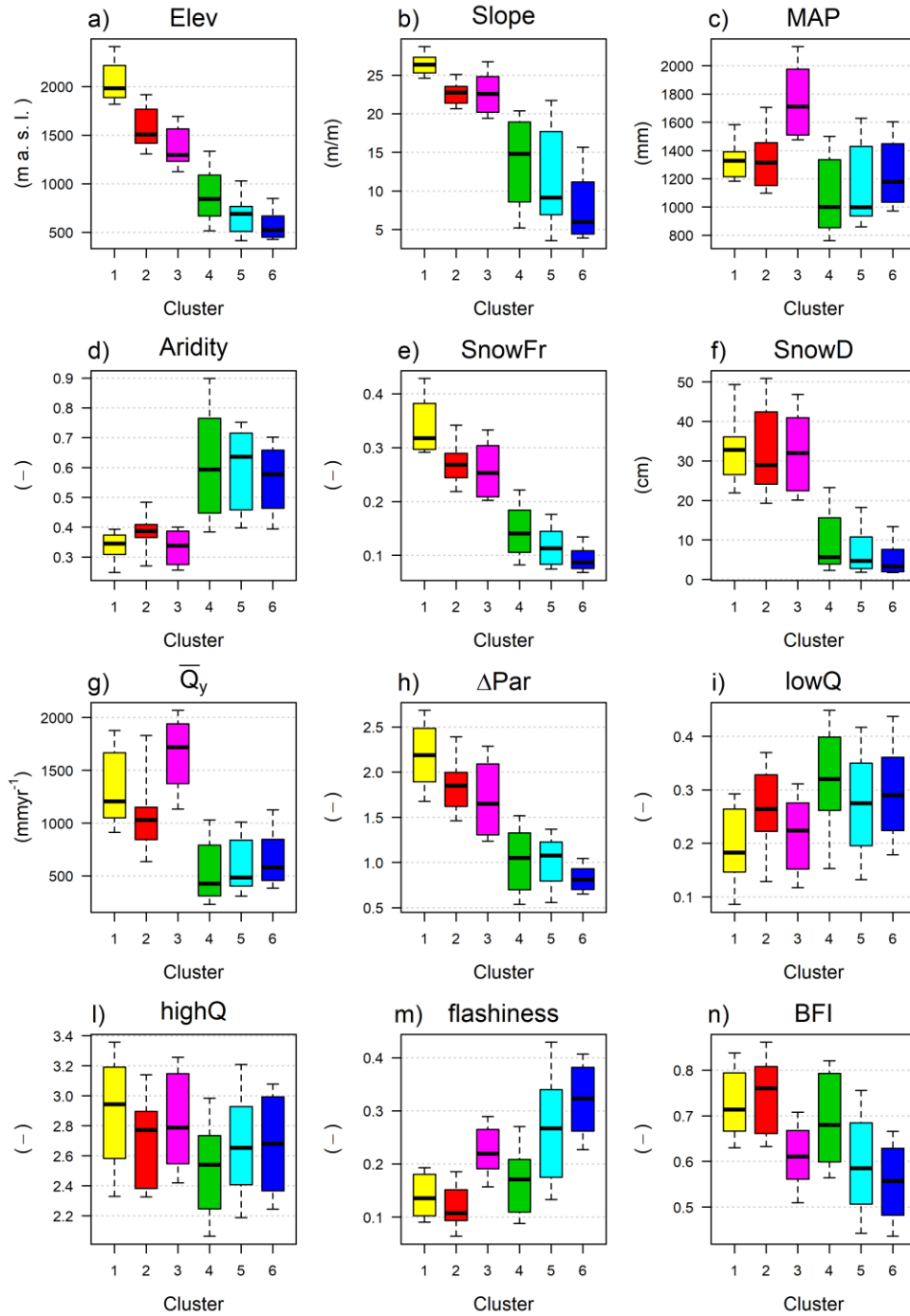


Figure 7. Variability of the morphological and climatic catchment attributes (elevation (a), slope (b), MAP (c), aridity index (d), snow fraction (e), snow depth (f) and streamflow signatures (mean annual runoff (g), range of Pardé's coefficients (h), low flow statistic (i), high flow statistic (l) flashiness index (m) and baseflow index (n)) inside the different clusters obtained through the TE-HC classification.

6 Discussion

6.1 Interpretation of the TE values

It is important to recall that when calculating the transfer entropy in the present formulation, we are estimating the impact (i.e. the net information flow) of the independent variables at the previous day. Looking first exclusively at the obtained transfer entropy (TE) values, it was observed that information flow from P reaches higher values than those from AET

and *melt* (Figure 2); in addition, the distributions of $TE_{AET \rightarrow Q}$ and $TE_{melt \rightarrow Q}$ are positively skewed. Such outcomes suggest that a 1-day lag precipitation signal can have a more direct impact on streamflow in comparison to the remaining runoff generation components, and that for the majority of the basins the information transferred from *AET* and *melt* signals on a previous day is less significant.

Beyond these first considerations, the interpretation of the resulting values of transfer entropy in the region is not straightforward and an additional understanding may be gained by analysing how the three TEs are individually linked to catchment attributes and streamflow features.

Looking at Figure 3, which shows the scatterplot between basin attributes and TE values, it can be noticed that $TE_{P \rightarrow Q}$ (first row) shows a substantial negative relation with mean elevation (*Elev*), mean slope (*Slope*), snow fraction (*SnowFr*) and snow depth (*SnowD*), which are also strongly correlated between each other (not explicitly showed here). Basins at high elevation, generally steeper and characterised by significant presence of snow, correspond to low values of transfer entropy from 1-day lag precipitation, while for decreasing altitudes (and decreasing *SnowFr* and *SnowD*) the range of variability of $TE_{P \rightarrow Q}$ increases and the relationship is less clear. The impact of *P* results to be negatively and significantly correlated also with some of the considered streamflow signatures (first row in Figure 4). ΔPar , which is a measure of catchment seasonality, shows the same kind of relationship as observed for elevation and presence of snow. In fact, seasonality in Austria is so much more influenced by snow accumulation and melting dynamics than by the seasonality of precipitation itself. Interestingly, the quickness of the runoff response, here quantified by the *flashiness* index, is positively correlated to the impact of the previous day's precipitation *P* with a Pearson's correlation coefficient of 0.67. In contrast, negative correlation of $TE_{P \rightarrow Q}$ to the baseflow index (*BFI*) is observed. This confirms that the information from 1-day lag precipitation is higher in catchments with the fastest runoff response, while it is weaker where additional dynamics (e.g. infiltration and snow dynamics) are involved. For what concerns the remaining streamflow and catchment features, even if more humid catchments usually correspond to higher values of mean annual runoff, the first rows of Figures 3 and 4 show that $TE_{P \rightarrow Q}$ correlates (even if weakly) with $\overline{Q_y}$ but it does not seem to be linked to *MAP*. Finally, no significant relations between *P* entropy values and low/high flow statistics (*lowQ* and *highQ*) are observed.

Given their high mutual correlation, $TE_{AET \rightarrow Q}$ and $TE_{melt \rightarrow Q}$ are linked in a similar way to morpho-climatic basin attributes and streamflow signatures (second and third rows in Figures 3 and 4). In contrast to the impact of *P*, they are positively correlated (Pearson's correlation between 0.6 and 0.7) with elevation and presence of snow, and flatter catchments corresponds in general to low impact of *AET* and *melt*. Mean annual precipitation (*MAP*), higher in mountainous basins due to the orographic component, is also positively correlated with the information flow from *melt* and more weakly with the impact of *AET* (Person's correlations equal to 0.63 and 0.43 respectively); in addition, more arid catchments are characterised by low information flow from actual evapotranspiration and snow melt. Consistently, high impact of such two components matches with high seasonality (ΔPar), which, as mentioned above, is one of primary characteristics of snow dominated catchments in Austria. They accumulate water in the form of snow during the autumn and winter and release it during spring and summer seasons, when snow melt occurs due to the temperature rise. Finally, 1 day-lag *AET* and especially *melt* TE are negatively correlated with low flow statistics (*lowQ*) and positively correlated with high flow statistics (*highQ*). In Austria in fact, seasonal and snow-dominated behaviour seems to be associated with more pronounced low and high flows as can be observed looking at their spatial pattern compared to that of ΔPar (Figure 6h-i-l). On one hand, snow deposition in the catchments instead of rain is responsible for small low flows, occurring in winter; on the other hand, the combination of high orographic precipitations and snow melt in spring and summer leads to particularly strong high flows in the more seasonal regions.

467 The results discussed so far show that the three considered transfer entropy variables alone are able to capture multiple
468 climatic, morphological and hydrological characteristics across the dataset. In general, from such first considerations we
469 can mainly observe that i) in Austria the differences in transfer entropy explain mainly those catchments' attributes and
470 streamflow signatures linked to snow accumulation and melting processes and that ii) the information transferred from
471 precipitation signal on a previous day is able to quantify the quickness of the runoff response.

472 6.2 Interpretation of the TE-HC classes

473 The proposed classification based on the transfer entropy values, here named TE-HC, eases the interpretation of the
474 results, merging the spatial pattern of the three signatures in a single map; in addition, considering a set of clusters instead
475 of single values allows one to highlight macro differences between catchments and to simplify the spatial pattern. As
476 mentioned previously, the results of the classification (illustrated in the upper portion of Figure 6) are analysed herein
477 against the spatial pattern of the morpho-climatic catchment attributes and streamflow signatures (below in the same
478 Figure 6). In addition, boxplots of Figure 7 show their values inside the clusters.

479 Looking at the results of the TE-HC, it can be first noticed how the methodology is able to capture and isolate the
480 catchments with the greatest amount of information flow from precipitation ($TE_{P \rightarrow Q}$). Cluster 5 and 6 (respectively light
481 and dark blue) group the catchments with the highest impact of P and low impact of AET and $melt$: these basins are
482 indeed typically flat and located at the lowest elevations (Figure 6a) where the presence of snow is not relevant (Figure
483 7a-b-e-f). Such clusters show consistently the highest *flashiness* index (Figure 6m and Figure 7m). At the same time,
484 they are characterised by the lowest baseflow (Figure 7n) and the lowest seasonality (Figure 7h). In the more flashy
485 catchments in fact, the delayed runoff components, due e.g. to groundwater release or snow seasonal dynamics, have low
486 influence and the runoff response is highly dependent on single rainfall events. Such hydrological behaviour is particularly
487 pronounced in the north-east and for a little area in the extreme west, corresponding with Cluster 6, which consistently
488 match the regions labelled as more “flashy” by previous studies, due to more convective precipitations and rapidly
489 draining soils (e.g. Gaál et al., 2012; Viglione et al., 2013).

490 Similar low information flow from AET and $melt$ but lower impact of P (even if still predominant on snow processes)
491 characterise Cluster 4 (green), located in the area at mid-low elevation, mainly in the south and in the east. Snow presence
492 is also low but, differently from Cluster 5 and 6, mean annual precipitation (Figure 7c) is the lowest and, consistently
493 with the lower impact of P , the hydrograph dynamics are slower (higher BFI and lower *flashiness*). In fact, Cluster 4
494 is mainly located in areas characterised by pervious soils (as highlighted by Viglione et al., 2013) where catchments are
495 typically able to self-regulate the runoff. For this reason, it shows also the highest low flows ($lowQ$, Figure 7i).

496 On the other hand, for Clusters 1 (yellow) and 2 (red), located along the Alps, the information flow from precipitation is
497 not predominant. In particular, for Cluster 1 the impact of 1 day-lag $melt$ and especially of AET , which is maximum,
498 exceeds that of P . It groups snow-dominated catchments located at the highest elevation, with the most pronounced
499 seasonality (Figure 7a-e-h). In fact, besides its direct effect on the water balance, transfer entropy from AET (highly
500 depending on temperature) may be linked also to the runoff seasonality: catchments with high seasonality have AET and
501 Q in phase during the year, while this is not valid in catchments with low seasonal behaviour. Consistently and as already
502 mentioned, the delayed snow dynamics lead such catchments to have the highest baseflow index (BFI). Cluster 2 includes
503 instead those Alpine catchments at slightly lower elevation with less extreme snowy and seasonal behaviour, where the
504 information flow from AET and $melt$ is similar to that from P . They are located mainly in the eastern part of the Alps.

505 Finally, Cluster 3 (magenta) is located in-between: it identifies catchments with strong impact of snow components, but
 506 where the information flow from precipitation is still prevalent: in fact, $TE_{AET \rightarrow Q}$ and $TE_{melt \rightarrow Q}$ are similar to those of
 507 Cluster 1, but at the same time $TE_{P \rightarrow Q}$ is stronger. Interestingly, these Alpine catchments are located exclusively on the
 508 northern side of the mountain chain, characterised by the highest annual precipitation of the country (Figure 6c and Figure
 509 7c), due as already mentioned to the orographic lifting of the north-western airflows, but where snow dynamics also
 510 strongly influence rainfall-runoff transformation processes (see e.g. Merz and Blöschl, 2009). In this region, the very high
 511 precipitations contribute on one side to a significant snow accumulation, but at the same time recent rainfall has had a
 512 direct impact on the runoff. In fact, even if MAP is so much higher than in the other Alpine catchments, snow
 513 accumulation ($SnowD$, Figure 7f) is still one of the largest in the region. With respect to the other Alpine catchments, the
 514 strong impact of 1-day lag P is reflected also in the stronger *flashiness* and slightly lower seasonality (Figure 7h-m).
 515 The identification of snow-dominated catchments (Clusters 1, 2 and 3) matches in general with those obtained by previous
 516 studies either based, e.g., on signatures (Viglione et al., 2013), on the drivers of flood timescales (Gaál et al., 2012) or on
 517 parameter sensitivity analysis (Sleziak et al., 2018).
 518 Looking overall at the pattern of TE components, catchment attributes and streamflow signatures, we observe increasing
 519 predominant impact of P compared to AET and $melt$ components moving from Cluster 1 to 6, corresponding to
 520 decreasing elevation and snow presence (Figure 7a-e-f), weaker seasonality and faster hydrograph dynamics (Figure 7h-
 521 m-n). In addition, even if Clusters 4 to 6 are characterised by a higher aridity index (Figure 7d) and a lower annual
 522 discharge (Figure 7g), they still show a much predominant impact of P . Moreover, even if we would expect a certain
 523 impact of evapotranspiration in such most arid catchments, the information flow from AET is actually the smallest: this
 524 may be due to the 1-day time lag considered for the experiment, hiding the slower contributions of the variable to the
 525 water balance. On the other hand, $\overline{Q_y}$ index is higher in Cluster 1 and 2 but it is maximum for Cluster 3 due to the highest
 526 orographic precipitations, consistently matching the larger $TE_{P \rightarrow Q}$ observed in the upper panel of Figure 6. Finally,
 527 differences in *lowQ* and *highQ* are not clearly highlighted through the TE classes (Figure 7i-l), except for Clusters 1 and
 528 3, characterised by the highest impact of AET and $melt$ and by a highly seasonal behaviour, which in Austria correspond
 529 also to weaker low flows and slightly stronger high flows.
 530 Overall it can be observed that the obtained classification, which relies exclusively on just three entropy-based quantities,
 531 is consistent with the values of basin attributes and streamflow signatures and with the overall interpretation of Austrian
 532 hydrology analysed in previous literature. In fact, this analysis demonstrated that information flows between rainfall-
 533 runoff drivers can be used as metrics for hydrological similarity.
 534 It has to be accepted that the study has a few limitations. The first is that transfer entropy values are calculated based on
 535 a single time lag, but on the other hand, the size of the basins is overall small. Secondly, since the purpose was to assess
 536 the potential of transfer entropy for catchment characterisation in the most parsimonious way, TE-HC was implemented
 537 considering information flow just from the three main meteorological forcing components and it can not take into account
 538 all the governing hydrological phenomena.
 539 Despite the limitations, the approach is able to distinguish the predominant or partial role of snow melt and
 540 evapotranspiration across the dataset. At the same time, the amount of information flow transferred from the precipitation
 541 to the runoff hydrograph, measuring the impact of rainfall events occurring in the previous day, can help on one side to
 542 highlight differences in catchment response time, but also to capture the direct effect of very high orographic precipitation
 543 on the runoff in mountain and snow dominated watersheds, as demonstrated by the delineation of Cluster 3 that groups
 544 the basins on the more humid side of the Alpine chain.

For such reasons, we believe that transfer entropy deserves further attention and investigation since it may be seen as an additional instrument to characterise catchment dynamics that are not fully captured by streamflow signatures alone, by providing a measure of the interaction between forcing variables and runoff.

7 Conclusions

A novel approach for the characterisation and classification of catchment dynamics through the quantification of the information flows between meteorological runoff forcings and runoff itself has been proposed. The central purpose of the analysis is to demonstrate the potential of transfer entropy measures for assessing the similarity in the main hydrological processes governing the rainfall-runoff transformation. Transfer entropy considers the interaction between each one of the entire meteorological forcing time series and it is able to quantify the amount of information transferred from them to the streamflow time series. The literature regarding catchment classification normally involves similarity measures based on different streamflow signatures or morphological and climatic features independently from each other. This work aimed to show how transfer entropy can be used as a complementary tool for identifying and highlighting similar catchment dynamics. This may be particularly interesting when the interaction between forcing variables and runoff needs to be understood, as for instance in the case of calibration and regionalisation of rainfall-runoff models. The information flow from i) measured daily precipitation ii) simulated actual evapotranspiration and iii) simulated snow melt to daily runoff time series was estimated through the computation of transfer entropy values. In order to avoid incurring further uncertainties due to the estimate of high-dimensional probability distributions and at the same time to simplify the transfer entropy calculation, thus allowing a better understanding of the information flow, transfer entropy was computed in this work considering only one previous time step (1 day-lag transfer entropy). Even though runoff is certainly affected by forcing variables at greater time lags, the analysis can still provide a first order estimate of the transfer entropy and of its ability in identifying useful catchment dynamics. Future analyses will indeed require the inclusion of higher time lags in transfer entropy computation, as well as the inclusion of further runoff forcing components as control variables, but this is beyond the scope of this pathfinder article. The obtained standardised transfer entropies were first analysed, comparing them to the values of available catchment attributes and to a set of six streamflow signatures, trying to better understand the results of the transfer entropy calculation. In general, the differences in transfer entropy tend to be partially explained by catchments features linked to orography, which plays a central role in the hydrological behaviour of catchments in such Alpine region, but at the same time it is noteworthy that the three transfer entropy metrics alone capture meaningful relationships with multiple descriptors and flow characteristics. Then, the transfer entropy values were used as catchment features when applying a hierarchical clustering algorithm. The rationale of the method is that similar values of information flow between meteorological forcing and streamflow time series mean similar catchment dynamics. Within the limitation of the study, the results of the classification are promising. The method is able to distinguish the predominant or partial role of snow melt and evapotranspiration across the dataset and, measuring the impact of rainfall events occurring in the previous day, it can help to highlight differences catchment response time and the role of very high orographic precipitation in snow-dominated catchments. The Transfer Entropy - Hierarchical Clustering (TE-HC), based exclusively on the three indices representing the interaction between forcings meteorological data and runoff, is consistent with the results of previous works (e.g. Gaál et al., 2012; Slezziak et al., 2018; Viglione et al., 2013) and with the pattern of the selected streamflow signatures and catchment attributes. The

methodology demonstrates its ability to capture similarity between more features of the runoff hydrograph described by the indices, and confirm therefore the useful contribution of information flow-based metrics.

The present analysis demonstrates the potential of TE-HC, and in particular the potential of transfer entropy, as an additional instrument for assessing hydrological similarity and for quantifying the connection between different processes. It deserves further investigation and should be seen as a complementary approach to classification techniques based on consolidated streamflow signatures. In particular, given that TE-HC is based on the concept of information flow between high-resolution forcing and streamflow time-series, it appears promising especially when the classification aims to detect similarity in dominant hydrological dynamics, like the transfer of rainfall-runoff model parameters, for instance. In fact, gauged classifications like TE-HC may help to train clustering algorithms based on basin attributes alone (as done e.g. by Jehn et al., 2020; McManamay and Derolph, 2019; Toth, 2013) in the ungauged case, or they can be directly implemented in regionalisation frameworks (e.g. Masih et al., 2010; Pool et al., 2021).

We trust that this work provides a platform for the extension of the ideas, and forthcoming experiments will focus on coupling the use of transfer entropy in catchment classification to the application of rainfall-runoff model regionalisation techniques, testing the improvement allowed by using such novel clusters as founding point of the regionalisation framework.

Appendix A: Table of the acronyms

Table 3. Table of the acronyms and their meaning.

Code	Description
<i>P</i>	Precipitation
<i>AET</i>	Actual evapotranspiration
<i>melt</i>	Snow melt
<i>Q</i>	Runoff
TE	Transfer entropy
TE-HC	Transfer Entropy – Hierarchical Clustering
<i>Elev</i>	Mean catchment elevation
<i>Slope</i>	Mean catchment slope
<i>MAP</i>	Mean annual total precipitation
<i>Aridity</i>	Aridity index
<i>SnowFr</i>	Fraction of precipitation fallen as snow (i.e. precipitation fallen in days below 0°)
<i>SnowD</i>	Mean annual snow depth
$\overline{Q_y}$	Mean annual specific runoff
ΔPar	Range of Parde's coefficients
<i>lowQ</i>	Normalised low flow statistic
<i>highQ</i>	Normalised high flow statistic
<i>flashiness</i>	Flashiness index
<i>BFI</i>	Baseflow index

Appendix B: Parameterisation of the TUW model

The sets of TUW model parameters are estimated for all the catchments with an automatic model calibration procedure, using the dynamically dimensioned search algorithm (DDS, Tolson and Shoemaker, 2007). The objective function to be maximised is the Kling–Gupta efficiency (Gupta et al., 2009) between observed and simulated streamflow.

All the available observation records (33 years) were entirely used for both model calibration and simulation, with a warm-up period of one year. We decided not to use a split-sample procedure, since the analysis of model performances

is not the aim of the present study and we know from the previous analyses (cited above) that the model behaves well in the study region. We preferred using the entire records both for estimating the model parameters and for simulating the snow melt and actual evapotranspiration state variables, in order to have the longest possible time series of the forcings for the computation of transfer entropy.

Table 4 lists TUW model parameters and the calibration ranges used in the study region. More detailed description of the meaning and the role of each of the parameter is available in Neri et al., (2020), together with a full description of model routines.

As mentioned in Sec. 4.1, TUW parameter ranges in Austria are set analogously to what done in previous applications of the same model (Neri et al., 2020; Parajka et al., 2005): 4 out of the 15 total parameters are pre-set, and 11 are calibrated: threshold temperatures T_R and T_S are fixed respectively to 2 and 0 °C, T_M to 0 °C and the maximum base of the transfer function at low flows B_{MAX} to 10 days.

Table 4. TUW model parameters and their calibration ranges for the study region.

Parameter	Description	Units	Range
SCF	Snow correction factor	-	0.9 – 1.5
DDF	Degree day factor	mm/°C/day	0 – 5
T_R	Threshold temperature above which precipitation is rain	°C	fixed to 2
T_S	Threshold temperature below which precipitation is snow	°C	fixed to 0
T_M	Threshold temperature above which melt starts	°C	fixed to 0
LP	Parameter related to the limit of evaporation	-	0 – 1
FC	Field capacity (i.e., max soil moisture storage)	Mm	0 – 600
β	Non linear parameter for runoff production	-	0 – 20
k_0	Storage coefficient for very fast response	days	0 – 2
k_1	Storage coefficient for fast response	days	2 – 30
k_2	Storage coefficient for slow response	days	30 – 250
L_{UZ}	Threshold storage state above which very fast response start	mm	0 – 100
C_{PERC}	Constant percolation rate	mm	0 – 8
B_{MAX}	Maximum base at low flows	days	fixed to 10
C_{ROUTE}	Scaling parameter	days ² /mm	fixed to 25

CRediT authorship contribution statement

Mattia Neri: Conceptualization, Methodology, Software, Validation, Formal analysis, Investigation, Writing - Original Draft, Writing - Review & Editing, Visualization. **Paulin Coulibaly:** Conceptualization, Methodology, Validation, Supervision. **Elena Toth:** Methodology, Validation, Investigation, Writing - Original Draft, Writing - Review & Editing, Supervision, Funding acquisition.

Declaration of Competing Interest

The authors declare that they have no known competing financial interests or personal relationships that could have appeared to influence the work reported in this paper.

Acknowledgements

The authors would like to thank Prof. Juraj Parajka (Institute for Hydraulic and Water Resources Engineering, Vienna University of Technology, Austria) for providing the hydro-meteorological data (daily streamflow and daily

631 meteorological time series) and the catchment features used in the work. We also thank the Editor, Prof. Geoff Pegram
 632 and an anonymous referee for their constructive comments and suggestions that have contributed to improve this paper.

633 References

- 634 Alfonso, L., Ridolfi, E., Gaytan-Aguilar, S., Napolitano, F., Russo, F., 2014. Ensemble Entropy for Monitoring
 635 Network Design. *Entropy* 16, 1365–1375. <https://doi.org/10.3390/e16031365>
- 636 Archfield, S.A., Kennen, J.G., Carlisle, D.M., Wolock, D.M., 2014. An Objective and Parsimonious Approach for
 637 Classifying Natural Flow Regimes at a Continental Scale. *River Research and Applications* 30, 1166–1183.
 638 <https://doi.org/10.1002/rra.2710>
- 639 Baker, D.B., Richards, R.P., Loftus, T.T., Kramer, J.W., 2004. A new flashiness index: characteristics and applications
 640 to Midwestern rivers and streams. *J Am Water Resources Assoc* 40, 503–522. <https://doi.org/10.1111/j.1752-1688.2004.tb01046.x>
- 641 Behrendt, S., Dimpfl, T., Peter, F.J., Zimmermann, D.J., 2019. RTransferEntropy — Quantifying information flow
 642 between different time series using effective transfer entropy. *SoftwareX* 10, 100265.
 643 <https://doi.org/10.1016/j.softx.2019.100265>
- 644 Ben Jaafar, A., Bargaoui, Z., 2020. Generalized Split-Sample Test Interpretation Using Rainfall Runoff Information
 645 Gain. *J. Hydrol. Eng.* 25, 04019057. [https://doi.org/10.1061/\(ASCE\)HE.1943-5584.0001868](https://doi.org/10.1061/(ASCE)HE.1943-5584.0001868)
- 646 Bennett, A., Nijssen, B., Ou, G., Clark, M., Nearing, G., 2019. Quantifying Process Connectivity With Transfer Entropy
 647 in Hydrologic Models. *Water Resources Research* 55, 4613–4629. <https://doi.org/10.1029/2018WR024555>
- 648 Berghuijs, W.R., Sivapalan, M., Woods, R.A., Savenije, H.H.G., 2014. Patterns of similarity of seasonal water
 649 balances: A window into streamflow variability over a range of time scales. *Water Resources Research* 50,
 650 5638–5661. <https://doi.org/10.1002/2014WR015692>
- 651 Bergström, S., 1976. Development and Application of a Conceptual Runoff Model for Scandinavian Catchments, A:
 652 Bulletin series. Department of Water Resources Engineering, Lund Institute of Technology, University of
 653 Lund.
- 654 Brunner, M., Melsen, L., Newman, A., Wood, A., Clark, M., 2020. Future streamflow regime changes in the United
 655 States: assessment using functional classification. *Hydrology and Earth System Sciences Discussions* 1–23.
 656 <https://doi.org/10.5194/hess-2020-54>
- 657 Budyko, M.I., 1974. *Climate and Life*. Academic Press, N. Y.
- 658 Castellarin, A., Burn, D.H., Brath, A., 2001. Assessing the effectiveness of hydrological similarity measures for flood
 659 frequency analysis. *Journal of Hydrology* 241, 270–285. [https://doi.org/10.1016/S0022-1694\(00\)00383-8](https://doi.org/10.1016/S0022-1694(00)00383-8)
- 660 Castiglioni, S., Lombardi, L., Toth, E., Castellarin, A., Montanari, A., 2010. Calibration of rainfall-runoff models in
 661 ungauged basins: A regional maximum likelihood approach. *Advances in Water Resources* 33, 1235–1242.
 662 <https://doi.org/10.1016/j.advwatres.2010.04.009>
- 663 Chiang, S.M., Tsay, T.K., Nix, S.J., 2002. Hydrologic regionalization of watersheds. I: Methodology development.
 664 *Journal of Water Resources Planning and Management* 128, 3–11. [https://doi.org/10.1061/\(ASCE\)0733-9496\(2002\)128:1\(3\)](https://doi.org/10.1061/(ASCE)0733-9496(2002)128:1(3))
- 665 Corduas, M., 2011. Clustering streamflow time series for regional classification. *Journal of Hydrology* 407, 73–80.
 666 <https://doi.org/10.1016/j.jhydrol.2011.07.008>
- 667 Cover, T.M., Thomas, J.A., 2005. Differential Entropy, in: *Elements of Information Theory*. John Wiley & Sons, Ltd,
 668 pp. 243–259. <https://doi.org/10.1002/047174882X.ch8>
- 669 De Thomasis, E., Grimaldi, S., 2001. Introduzione di una metrica tra modelli parametrici lineari nelle applicazioni di
 670 tipo idrologico, in: *Giornata Di Studio: Metodi Statistici and Matematici per l'Analisi Delle Serie Idrologiche*,
 671 Roma.
- 672 Ehret, U., van Pruijssen, R., Bortoli, M., Loritz, R., Azmi, E., Zehe, E., 2020. Adaptive clustering: reducing the
 673 computational costs of distributed (hydrological) modelling by exploiting time-variable similarity among
 674 model elements. *Hydrol. Earth Syst. Sci.* 24, 4389–4411. <https://doi.org/10.5194/hess-24-4389-2020>
- 675 Fahle, M., Hohenbrink, T.L., Dietrich, O., Lischeid, G., 2015. Temporal variability of the optimal monitoring setup
 676 assessed using information theory. *Water Resources Research* 51, 7723–7743.
 677 <https://doi.org/10.1002/2015WR017137>
- 678 Foroozand, H., Weijs, S.V., 2021. Objective functions for information-theoretical monitoring network design: what is
 679 “optimal”? *Hydrol. Earth Syst. Sci.* 25, 831–850. <https://doi.org/10.5194/hess-25-831-2021>
- 680 Gaál, L., Szolgay, J., Kohnová, S., Parajka, J., Merz, R., Viglione, A., Blöschl, G., 2012. Flood timescales:
 681 Understanding the interplay of climate and catchment processes through comparative hydrology: FLOOD
 682 TIMESCALES AND COMPARATIVE HYDROLOGY. *Water Resour. Res.* 48.
 683 <https://doi.org/10.1029/2011WR011509>
- 684 Grimaldi, S., 2004. Linear Parametric Models Applied to Daily Hydrological Series. *Journal of Hydrologic Engineering*
 685 9, 383–391. [https://doi.org/10.1061/\(ASCE\)1084-0699\(2004\)9:5\(383\)](https://doi.org/10.1061/(ASCE)1084-0699(2004)9:5(383))

688 Gupta, H.V., Kling, H., Yilmaz, K.K., Martinez, G.F., 2009. Decomposition of the mean squared error and NSE
689 performance criteria: Implications for improving hydrological modelling. *Journal of Hydrology* 377, 80–91.
690 <https://doi.org/10.1016/j.jhydrol.2009.08.003>

691 Gustard, A., Bullock, A., Dixon, J.M., 1992. Low Flow Estimation in the United Kingdom (No. 108). Institute of
692 Hydrology, Wallingford, UK.

693 Hall, F.R., 1968. Base-Flow Recessions-A Review. *Water Resour. Res.* 4, 973–983.
694 <https://doi.org/10.1029/WR004i005p00973>

695 Hlinka, J., Hartman, D., Vejmelka, M., Runge, J., Marwan, N., Kurths, J., Paluš, M., 2013. Reliability of Inference of
696 Directed Climate Networks Using Conditional Mutual Information. *Entropy* 15, 2023–2045.
697 <https://doi.org/10.3390/e15062023>

698 Holmes, M.G.R., Young, A.R., Gustard, A., Grew, R., 2002. A new approach to estimating Mean Flow in the UK.
699 *Hydrology and Earth System Sciences* 6, 709–720. <https://doi.org/10.5194/hess-6-709-2002>

700 Jehn, F.U., Bestian, K., Breuer, L., Kraft, P., Houska, T., 2020. Using hydrological and climatic catchment clusters to
701 explore drivers of catchment behavior. *Hydrology and Earth System Sciences* 24, 1081–1100.
702 <https://doi.org/10.5194/hess-24-1081-2020>

703 Keum, J., Coulibaly, P., 2017. Information theory-based decision support system for integrated design of multivariable
704 hydrometric networks. *Water Resources Research* 53, 6239–6259. <https://doi.org/10.1002/2016WR019981>

705 Keum, J., Kornelsen, K.C., Leach, J.M., Coulibaly, P., 2017. Entropy applications to water monitoring network design:
706 A review. *Entropy* 19, 1–21. <https://doi.org/10.3390/e19110613>

707 Knoben, W.J.M., Woods, R.A., Freer, J.E., 2018. A Quantitative Hydrological Climate Classification Evaluated With
708 Independent Streamflow Data. *Water Resources Research* 54, 5088–5109.
709 <https://doi.org/10.1029/2018WR022913>

710 Krstanovic, P.F., Singh, V.P., 1992. Evaluation of rainfall networks using entropy: II. Application. *Water Resources*
711 *Management* 6, 295–314. <https://doi.org/10.1007/BF00872282>

712 Kuentz, A., Arheimer, B., Hundecha, Y., Wagener, T., 2017. Understanding hydrologic variability across Europe
713 through catchment classification. *Hydrology and Earth System Sciences* 21, 2863–2879.
714 <https://doi.org/10.5194/hess-21-2863-2017>

715 Laaha, G., Blöschl, G., 2006. A comparison of low flow regionalisation methods-catchment grouping. *Journal of*
716 *Hydrology* 323, 193–214. <https://doi.org/10.1016/j.jhydrol.2005.09.001>

717 Lindström, G., Johansson, B., Persson, M., Gardelin, M., Bergström, S., 1997. Development and test of the distributed
718 HBV-96 hydrological model. *Journal of Hydrology* 201, 272–288. [https://doi.org/10.1016/S0022-1694\(97\)00041-3](https://doi.org/10.1016/S0022-1694(97)00041-3)

719 Lombardi, L., Toth, E., Castellarin, A., Montanari, A., Brath, A., 2012. Calibration of a rainfall-runoff model at regional
720 scale by optimising river discharge statistics: Performance analysis for the average/low flow regime. *Physics*
721 *and Chemistry of the Earth, Parts A/B/C* 42–44, 77–84. <https://doi.org/10.1016/j.pce.2011.05.013>

722 Loritz, R., Gupta, H., Jackisch, C., Westhoff, M., Kleidon, A., Ehret, U., Zehe, E., 2018. On the dynamic nature of
723 hydrological similarity. *Hydrology and Earth System Sciences* 22, 3663–3684. <https://doi.org/10.5194/hess-22-3663-2018>

724 Marschinski, R., Kantz, H., 2002. Analysing the information flow between financial time series. *The European Physical*
725 *Journal B* 30, 275–281. <https://doi.org/10.1140/epjb/e2002-00379-2>

726 Masih, I., Uhlenbrook, S., Maskey, S., Ahmad, M.D., 2010. Regionalization of a conceptual rainfall-runoff model based
727 on similarity of the flow duration curve: A case study from the semi-arid Karkheh basin, Iran. *Journal of*
728 *Hydrology* 391, 188–201. <https://doi.org/10.1016/j.jhydrol.2010.07.018>

729 McManamay, R.A., Derolph, C.R., 2019. Data descriptor: A stream classification system for the conterminous United
730 States. *Scientific Data* 6, 1–18. <https://doi.org/10.1038/sdata.2019.17>

731 Merz, R., Blöschl, G., 2009. A regional analysis of event runoff coefficients with respect to climate and catchment
732 characteristics in Austria: REGIONAL ANALYSIS OF EVENT RUNOFF COEFFICIENTS. *Water Resour.*
733 *Res.* 45. <https://doi.org/10.1029/2008WR007163>

734 Merz, R., Blöschl, G., 2005. Flood frequency regionalisation: spatial proximity vs. catchment attributes. *Journal of*
735 *Hydrology* 302, 283–306. <https://doi.org/10.1016/j.jhydrol.2004.07.018>

736 Merz, R., Blöschl, G., 2004. Regionalisation of catchment model parameters. *Journal of Hydrology* 287, 95–123.
737 <https://doi.org/10.1016/j.jhydrol.2003.09.028>

738 Mészáros, I., Miklánec, P., Parajka, J., 2002. Solar energy income modelling in mountainous areas. *Interdisciplinary*
739 *Approaches in Small Catchment Hydrology: Monitoring and Research - Proceedings of the 9th Conference of*
740 *the European Network of Experimental and Representative Basins* 127–135.

741 Mishra, A.K., Coulibaly, P., 2009. Developments in hydrometric network design: A review. *Reviews of Geophysics* 47.
742 <https://doi.org/10.1029/2007RG000243>

743 Montanari, A., Toth, E., 2007. Calibration of hydrological models in the spectral domain: An opportunity for scarcely
744 gauged basins? *Water Resources Research* 43. <https://doi.org/10.1029/2006WR005184>

745 Natural Environment Research Council, 1980. Low Flow Studies Report no.1 Research Report. Institute of Hydrology,
746 Wallingford, UK.

749 Neri, M., Parajka, J., Toth, E., 2020. Importance of the informative content in the study area when regionalising
750 rainfall-runoff model parameters: the role of nested catchments and gauging station density. *Hydrology and*
751 *Earth System Sciences* 24, 5149–5171. <https://doi.org/10.5194/hess-24-5149-2020>

752 Neuper, M., Ehret, U., 2019. Quantitative precipitation estimation with weather radar using a data- and information-
753 based approach. *Hydrol. Earth Syst. Sci.* 23, 3711–3733. <https://doi.org/10.5194/hess-23-3711-2019>

754 Ozkul, S., Harmancioglu, N.B., Singh, V.P., 2000. Entropy-Based Assessment of Water Quality Monitoring Networks.
755 *Journal of Hydrologic Engineering* 5, 90–100. [https://doi.org/10.1061/\(ASCE\)1084-0699\(2000\)5:1\(90\)](https://doi.org/10.1061/(ASCE)1084-0699(2000)5:1(90))

756 Parajka, J., Merz, R., Blöschl, G., 2005. A comparison of regionalisation methods for catchment model parameters.
757 *Hydrology and Earth System Sciences* 9, 157–171. <https://doi.org/10.5194/hess-9-157-2005>

758 Parajka, J., Merz, R., Blöschl, G., 2003. Estimation of daily potential evapotranspiration for regional water balance
759 modeling in Austria, in: 11th International Poster Day and Institute of Hydrology Open Day "Transport of
760 Water, Chemicals and Energy in the Soil - Crop Canopy - Atmosphere System". Slovak Academy of Sciences,
761 Bratislava, pp. 299–306.

762 Pérez Ciria, T., Chiogna, G., 2020. Intra-catchment comparison and classification of long-term streamflow variability in
763 the Alps using wavelet analysis. *Journal of Hydrology* 587, 124927.
764 <https://doi.org/10.1016/j.jhydrol.2020.124927>

765 Pool, S., Vis, M., Seibert, J., 2021. Regionalization for Ungauged Catchments — Lessons Learned From a Comparative
766 Large-Sample Study. *Water Res* 57. <https://doi.org/10.1029/2021WR030437>

767 R Core Team, 2019. R: A Language and Environment for Statistical Computing. R Foundation for Statistical
768 Computing, Vienna, Austria.

769 Rajsekhar, D., Mishra, A.K., Singh, V.P., 2013. Regionalization of drought characteristics using an entropy approach.
770 *Journal of Hydrologic Engineering* 18, 870–887. [https://doi.org/10.1061/\(ASCE\)HE.1943-5584.0000683](https://doi.org/10.1061/(ASCE)HE.1943-5584.0000683)

771 Rao, A.R., Srinivas, V.V., 2006. Regionalization of watersheds by fuzzy cluster analysis. *Journal of Hydrology* 318,
772 57–79. <https://doi.org/10.1016/j.jhydrol.2005.06.004>

773 Ridolfi, E., Rianna, M., Trani, G., Alfonso, L., Di Baldassarre, G., Napolitano, F., Russo, F., 2016. A new methodology
774 to define homogeneous regions through an entropy based clustering method. *Advances in Water Resources* 96,
775 237–250. <https://doi.org/10.1016/j.advwatres.2016.07.007>

776 Rosbjerg, D., Blöschl, G., Burn, D., Castellarin, A., Croke, B., Di Baldassarre, G., Iacobellis, V., Kjeldsen, T.R.,
777 Kuczera, G., Merz, R., Montanari, A., Morris, D., Ouara, T.B.M.J., Ren, L., Rogger, M., Salinas, J.L., Toth,
778 E., Viglione, A., 2013. Prediction of floods in ungauged basins, in: Blöschl, G., Sivapalan, M., Wagener, T.,
779 Viglione, A., Savenije, H. (Eds.), *Runoff Prediction in Ungauged Basins: Synthesis across Processes, Places*
780 *and Scales*. Cambridge University Press, Cambridge, pp. 189–226.
781 <https://doi.org/10.1017/CBO9781139235761.012>

782 Ruddell, B.L., Kumar, P., 2009. Ecohydrologic process networks: 2. Analysis and characterization. *Water Resources*
783 *Research* 45. <https://doi.org/10.1029/2008WR007280>

784 Sawicz, K., Wagener, T., Sivapalan, M., Troch, P.A., Carrillo, G., 2011. Catchment classification: empirical analysis of
785 hydrologic similarity based on catchment function in the eastern USA. *Hydrology and Earth System Sciences*
786 15, 2895–2911. <https://doi.org/10.5194/hess-15-2895-2011>

787 Schreiber, T., 2000. Measuring Information Transfer. *Physical Review Letters* 85, 461–464.
788 <https://doi.org/10.1103/PhysRevLett.85.461>

789 Shannon, C.E., 1948. A mathematical theory of communication. *The Bell System Technical Journal* 27, 379–423.
790 <https://doi.org/10.1002/j.1538-7305.1948.tb01338.x>

791 Sikorska, A.E., Viviroli, D., Seibert, J., 2015. Flood-type classification in mountainous catchments using crisp and
792 fuzzy decision trees. *Water Resour. Res.* 51, 7959–7976. <https://doi.org/10.1002/2015WR017326>

793 Singh, S.K., McMillan, H., Bárdossy, A., Fateh, C., 2016. Nonparametric catchment clustering using the data depth
794 function. *Hydrological Sciences Journal* 61, 2649–2667. <https://doi.org/10.1080/02626667.2016.1168927>

795 Singh, V.P., 1997. The use of entropy in hydrology and water resources. *Hydrological Processes* 11, 587–626.
796 [https://doi.org/10.1002/\(SICI\)1099-1085\(199705\)11:6<587::AID-HYP479>3.0.CO;2-P](https://doi.org/10.1002/(SICI)1099-1085(199705)11:6<587::AID-HYP479>3.0.CO;2-P)

797 Slezziak, P., Szolgay, J., Hlavčová, K., Duethmann, D., Parajka, J., Danko, M., 2018. Factors controlling alterations in
798 the performance of a runoff model in changing climate conditions. *Journal of Hydrology and Hydromechanics*
799 66, 381–392. <https://doi.org/10.2478/johh-2018-0031>

800 Swain, J.B., Patra, K.C., 2019. Impact of catchment classification on streamflow regionalization in ungauged
801 catchments. *SN Applied Sciences* 1, 456. <https://doi.org/10.1007/s42452-019-0476-6>

802 Tarasova, L., Basso, S., Wendi, D., Viglione, A., Kumar, R., Merz, R., 2020. A Process-Based Framework to
803 Characterize and Classify Runoff Events: The Event Typology of Germany. *Water Resour. Res.* 56.
804 <https://doi.org/10.1029/2019WR026951>

805 Thiesen, S., Vieira, D.M., Mälicke, M., Loritz, R., Wellmann, J.F., Ehret, U., 2020. Histogram via entropy reduction
806 (HER): an information-theoretic alternative for geostatistics. *Hydrol. Earth Syst. Sci.* 24, 4523–4540.
807 <https://doi.org/10.5194/hess-24-4523-2020>

808 Tolson, B.A., Shoemaker, C.A., 2007. Dynamically dimensioned search algorithm for computationally efficient
809 watershed model calibration. *Water Resources Research* 43. <https://doi.org/10.1029/2005WR004723>

810 Toth, E., 2013. Catchment classification based on characterisation of streamflow and precipitation time series.
811 Hydrology and Earth System Sciences 17, 1149–1159. <https://doi.org/10.5194/hess-17-1149-2013>
812 Vezza, P., Comoglio, C., Rosso, M., 2010. Low Flows Regionalization in North-Western Italy. Water Resources
813 Management 24, 4049–4074. <https://doi.org/10.1007/s11269-010-9647-3>
814 Viglione, A., Claps, P., Laio, F., 2007. Mean annual runoff estimation in North-Western Italy, in: La Loggia, G.,
815 Aronica, G.T., Ciruolo, G. (Eds.), Water Resources Assessment and Management under Water Scarcity
816 Scenarios. Centro Studi Idraulica Urbana, Torino, pp. 97–122.
817 Viglione, A., Parajka, J., 2018. TUWmodel: Lumped Hydrological Model for Education Purposes.
818 Viglione, A., Parajka, J., Rogger, M., Salinas, J.L., Laaha, G., Sivapalan, M., Blöschl, G., 2013. Comparative
819 assessment of predictions in ungauged basins - Part 3: Runoff signatures in Austria. Hydrology and Earth
820 System Sciences 17, 2263–2279. <https://doi.org/10.5194/hess-17-2263-2013>
821 Ward, J.H., 1963. Hierarchical Grouping to Optimize an Objective Function. Journal of the American Statistical
822 Association 58, 236–244. <https://doi.org/10.1080/01621459.1963.10500845>
823 Yaeger, M., Coopersmith, E., Ye, S., Cheng, L., Viglione, A., Sivapalan, M., 2012. Exploring the physical controls of
824 regional patterns of flow duration curves – Part 4: A synthesis of empirical analysis, process modeling
825 and catchment classification. Hydrology and Earth System Sciences 16, 4483–4498.
826 <https://doi.org/10.5194/hess-16-4483-2012>
827